International Journal of Technology 15(2) 373-382 (2024)
Received July 2023 / Revised September 2023 / Accepted November 2023

International Journal of Technology

http://ijtech.eng.ui.ac.id

Synthesis of Mesoporous Silica from Sugarcane Bagasse as Adsorbent for Colorants Using Cationic and Non-Ionic Surfactants

Donanta Dhaneswara[1,2*], Audrey Tsania[1], Jaka Fajar Fatriansyah[1,2], Andreas Federico[1,2], Ratu Ulfiati[3], Rifai Muslih[4], Mohd Sufri Mastuli[5,6]

[1]*Department of Metallurgical and Materials Engineering, Faculty of Engineering, Universitas Indonesia, Kampus UI Depok, Jawa Barat, 16242, Indonesia*
[2]*Advanced Materials Research Center (AMRC), Faculty of Engineering, Universitas Indonesia, Kampus UI Depok, Jawa Barat 16424, Indonesia*
[3]*Research Center for Process and Manufacturing Industrial Technology, National Research and Innovation Agency (BRIN), Klaster Teknologi Energi, Kawasan Puspiptek, Banten 15314, Indonesia*
[4]*Nuclear Energy Research Organization, National Research and Innovation Agency (BRIN), Kawasan Puspiptek, Banten 15314, Indonesia*
[5]*School of Chemistry and Environment, Faculty of Applied Sciences, Unversiti Teknologi MARA, 40450 Shah Alam Selangor, Malaysia*
[6]*Centre for Functional Materials and Nanotechnology, Institute of Science, Universiti Teknologi MARA, 40450 Shah Alam, Selangor, Malaysia*

Abstract. In Indonesia, the rising sugar production contributes to an increase in sugarcane bagasse waste. This waste can be used for environmental purposes, such as the treatment of colorants in the textile industry using mesoporous silica materials. Previous studies showed the potential of synthesizing mesoporous silica from agricultural waste including corn cob and rice husk. Therefore, this study aimed to investigate the potential use of sugarcane bagasse as an alternative waste source for synthesizing mesoporous silica. Sugarcane bagasse ash, containing a high silica content ranging from 55.5% to 70%, served as the main silica source for synthesis. A combination of surfactant templates, Pluronic 123 (P123), and Cetyl Trimethyl Ammonium Bromide (CTAB) in a ratio of 1:1, was used to obtain optimal structure, surface area, pore radius, and pore volume. These parameters were optimized to enhance the adsorption of colorants, specifically methyl blue commonly found in textile waste. The characterization techniques used included Small-Angle X-ray Scattering (SAXS), Scanning Electron Microscopy (SEM), Fourier Transform Infrared Spectroscopy (FTIR), Brunauer-Emmett-Teller (BET) analysis, and UV-Vis spectroscopy. The synthesized mesoporous silica showed a surface area of 323.3 m^2/g, a pore radius of 2.437 Å, and a pore volume of 0.52 cc/g, with an adsorption capacity of 97.3%. This adsorbent product was expected to provide a cost-effective, eco-friendly source of silica suitable for various dye adsorption applications and the treatment of heavy metals in industrial waste.

Keywords: Mesoporous silica; Organic colorants; Sugarcane bagasse ash; Surfactant

1. Introduction

Indonesia is one of the largest producers of agricultural commodities globally, including sugarcane, with a production of 2.4 million tons in 2022. The high quantity of

*Corresponding author's email: donanta.dhaneswara@ui.ac.id, Tel.: +62-813-1680-3755
doi: 10.14716/ijtech.v15i2.6721

sugarcane crop production results in a large amount of processing activities, leading to greater bagasse production as by-product. To increase the added value of bagasse waste, an appropriate processing strategy is needed by observing the potential use.

Bagasse waste can be burned to ash with high silica content ranging from 55.5 to 70% (Wilson and Mahmud, 2015). This phenomenon presents a significant use of bagasse waste, specifically in the creation of mesoporous ceramic material (Szewczyk and Prokopowicz, 2020), characterized by a high surface area suitable for adsorption purposes. Generally, adsorbent materials can be used in various applications, such as in drug delivery systems, oil adsorption, heavy metals, and dyes (Sohrabnezhad, Jafarzadeh, and Pourahmad, 2018; Bulgariu and Bulgariu, 2018).

The application of adsorbent for dye removal is based on the urgent need to overcome the environmental impact of azo dyes produced by textile industry waste (Sudibandriyo and Putri, 2020; Jawad *et al*. 2020; Mota *et al.,* 2019). Moreover, the use of mesoporous silica material as an adsorbent has shown good adsorption performance. Raya *et al.* (2021) conducted adsorption testing of azo dyes methylene blue using tetraethyl orthosilicate (TEOS)-based mesoporous silica material. The results showed a significant MB removal percentage of 96.27% for 3 h adsorption of 100 ppm MB. However, the use of silica material could be more efficient, considering that TEOS raw materials are expensive, leading to high product costs. Thu *et al.* (2019) fabricated rice husk biomass waste-based mesoporous silica material to overcome the problem, but the adsorption performance was not that high. To enhance the adsorption performance of mesoporous silica material, one promising solution is the addition of other surfactants as cosurfactants. Dhaneswara *et al.* (2023) observed the effect of Pluronic 123 (P123) and Cetyl Trimethyl Ammonium Bromide (CTAB) surfactant ratio on the adsorption performance of methylene blue, methyl orange on rice husk, and corn cob based mesoporous silica. The result yielded a maximum adsorption and surface area at a P123 and CTAB ratio of 1:1.

This study aimed to synthesize mesoporous silica derived from sugarcane bagasse using the sol-gel method and testing the adsorption capacity of methyl blue. The analysis was conducted to investigate typesetting P123 and CTAB surfactants as templates and the interaction process between surfactant and precursor silica sources. The product of mesoporous silica was characterized by Small-Angle X-ray Scattering (SAXS), Scanning Electron Microscopy (SEM), Fourier Transform Infrared Spectroscopy (FTIR), Brunauer-Emmett-Teller (BET) analysis, and UV-Vis spectroscopy.

2. Materials and Methods

The material used in this study included silica precursor raw material derived from sugarcane bagasse obtained at a plantation in Blitar, East Java. The surfactants used as templates were CTAB with a quantity of 7.5 g (Sigma-Aldrich) and P123 of 7.5 g (Sigma-Aldrich). Hydrochloric acid (HCl) solution (Supelco) was used as the acid solution, while sodium hydroxide (Supelco) was applied as the base solution. Subsequently, all chemicals passed through processes such as dilution and dissolution.

2.1. Synthesis Silica Mesoporous

Synthesis of mesoporous silica commenced with the extraction of silica precursor from sugarcane bagasse ash (SCBA) using a NaOH alkaline solvent (Fatriansyah Situmorang, and Dhaneswara, 2018; Shah *et al.,* 2017), which resulted in sodium silicate (Na_2SiO_3) as the product (Equation 1). P123 and CTAB surfactants were dissolved in an acid solution with continuous stirring and added with Na_2SO_3 dropwisely. Subsequently, stirring was continued at 28°C for 2 hours, followed by aging at 40°C for 24 hours, resulting in hydrolysis

and condensation of silica, as shown in Equations 2 and 3 (Sohrabnezhad, Jafarzadeh, and Pourahmad, 2018). After the gel was formed, the gel was dried, followed by calcination at 550°C for 5 h.

$$SiO_2(s) + 2NaOH\,(aq) \rightarrow Na_2SiO_3(aq) + H_2O\,(aq) \quad (1)$$

$$Na_2SiO_3 + x\,H_2O + 2H + \rightarrow SiO_2(x+1)H_2O + 2Na^+ \quad (2)$$

$$Si - OH + Si + \rightarrow Si - O - Si + H + (x) \quad (3)$$

2.2. Characterization

Synthesized mesoporous silica was characterized to determine its pore structure, morphology, and adsorption capacity. The crystal structure and orientation of mesoporous silica were characterized by SAXS Shimadzu XRD 6000 using CuKα radiation (1.54 Å wavelength) at a diffraction angle (2θ) ranging from 0.2 to 5°. Subsequently, the surface morphology and particle shape of mesoporous silica were observed using field emission scanning electron microscope (FE-SEM) FEI Inspect F50. The observation was performed at magnifications of 5000x and 10,000x. The functional groups present were determined using FTIR spectroscopy PerkinElmer in the infrared adsorption wavelength (500-4000 cm^{-1}). The pore structure and characterization were evaluated using Quantachrome NOVA 1200e BET nitrogen adsorption with the Barret-Joyner-Halenda (BJH) method. Finally, the adsorption performance of mesoporous silica in MB was tested using Lambda 25 PerkinElmer UV-Vis spectroscopy with wavenumbers ranging from 500 to 700 nm. The graph of the test results was used as a reference to determine the adsorption capacity (qt) of mesoporous silica and the percentage of methyl blue dye removed from the solution (%removal) each hour using Equations (4) and (5):

$$qt = \frac{(Co - Ct)\,V}{m} \quad (4)$$

$$\%Removal = \frac{(Co - Ct)}{Co} \quad (5)$$

Where C_t and C_o represent the concentrations of the Blanco solution, and the dye solution adsorbed during a certain time, while A_o and A_t shows the absorbance intensities of the Blanco solution and the dye solution adsorbed during a certain time. qt represents the uptake capacity at time t ($mg.g^{-1}$), m is the mass of the adsorbent (g), and V is the volume (Dhaneswara *et al.*, 2022).

3. Results and Discussion

3.1. Identification of Crystal Structure

Synthesized mesoporous silica sample was subjected to SAXS testing and the pattern obtained was shown in Figure 1. From the curve, an intense peak was observed at 1.2° and less intense peaks at 0.85° and 2°, representing (110), (200), and (211) planes, respectively. This confirmed the long-range order mesostructure of mesoporous silica (Dhaneswara *et al.*, 2022).

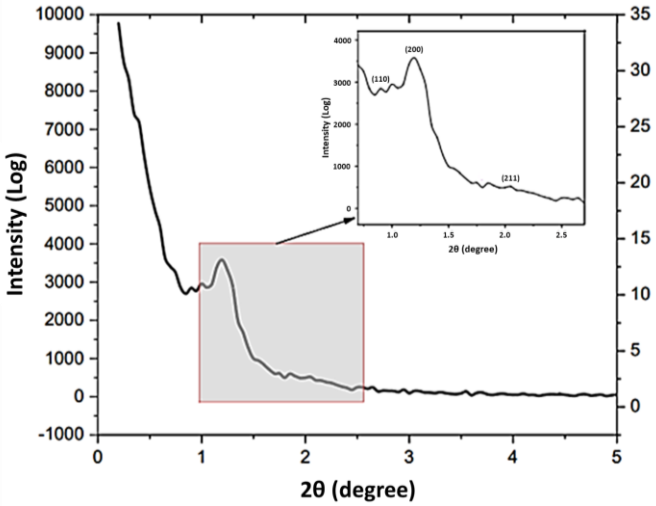

Figure 1 SAXS patterns for SCBA mesoporous

3.2. Surface Morphology

Based on the data from SEM analysis shown in Figure 2 at magnifications of 5000x and 10,000x, it was observed that mesoporous material synthesized using silica precursor from sugarcane bagasse adopted a spherical geometry. The properties of P123 lead to the formation of coarse aggregates among the perfectly agglomerated spherical particles. According to the literature, a surfactant ratio of 1:1 between CTAB and P123 resulted in the formation of perfectly agglomerated spherical particles. This ratio allows CTAB in P123 surfactant to influence the particle morphology through the formed micelles (Henao *et al.,* 2020). The role of CTAB includes dehydrating the polypropylene oxide (PPO) groups on the carbon chain, and reducing the hydrophobic volume of the micelles (Henao *et al.,* 2020). The reduction in PPO chains contributes to an increase in the ah/ac value in the packing parameters of the micelle, where ah represents the effective area of the hydrophilic chain, and as is the length of the hydrophobic chain (Nassar, Ahmed, and Raya, 2019). When CTAB concentration increases, resulting particles tend to adopt a spherical shape due to the interconnection of the hydrophobic alkyl chains, followed by the hydrophilic heads that have bonded with silica, merging and forming a bilayer (Nassar, Ahmed, and Raya, 2019). Consequently, SEM results suggest the presence of a few coarse aggregates due to an excessive concentration of P123. These coarse aggregates may be attributed to inaccuracies in weighing the P123 surfactant, which should be in a 1:1 ratio between P123 and CTAB. In addition to SEM, the morphology of mesoporous silica was also observed by using TEM, as shown in Figure 3. TEM images confirmed that mesoporous silica showed the ordered pore structure in the radial arrangement, showing the spherical-shaped particles (Abboud *et al.,* 2020).

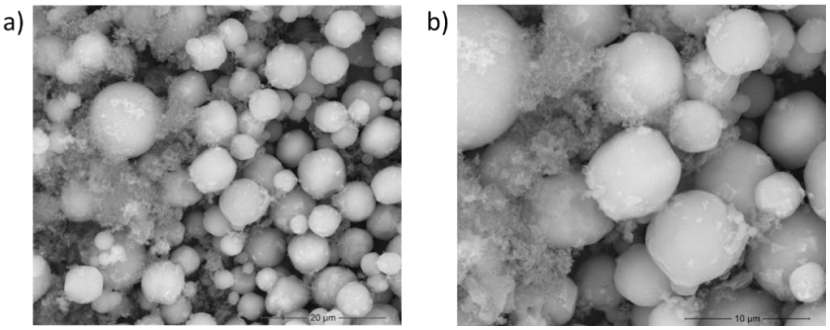

Figure 2 SEM images of SCBA Mesoporous: (a) 5000x magnification and (b) 10,000x magnification

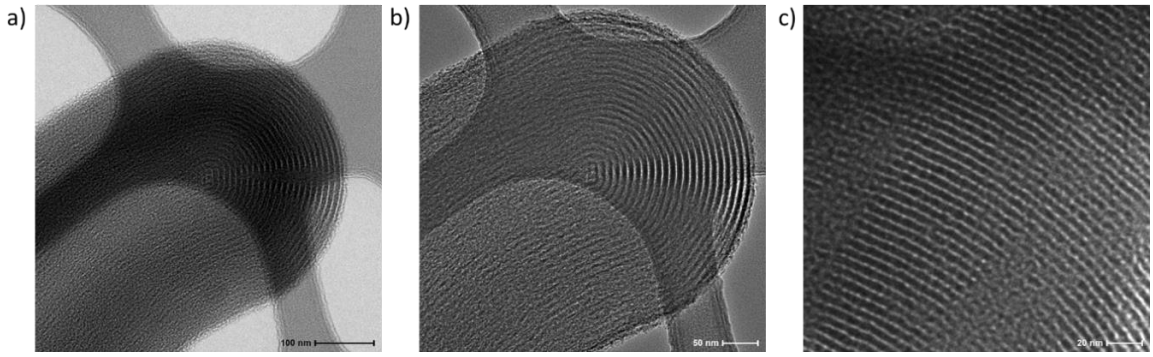

Figure 3 TEM images of the obtained SCBA mesoporous at: (a) x 100 nm, (b) x 50 nm, and (c) x 20 nm magnification

3.3. Adsorption-Desorption Curve

In BET analysis, the results showed crucial parameters such as surface area, pore radius, and pore volume of mesoporous silica material derived from sugarcane bagasse. This analysis also served to confirm the structural characteristics of a material through the formation of the adsorption-desorption isotherm curve, as shown in Figure 4. Synthesized mesoporous silica using sugarcane bagasse precursor tends to show Type IV in the classification of the adsorption isotherm curve according to IUPAC (Pingarrón *et al.,* 2020). Type IV showed that the resulting mesoporous silica had mesopores. characterized by an almost horizontal line in the high relative pressure region. Meanwhile, when mesoporous adsorbate contained macropores, the horizontal line would not form (Wang *et al.,* 2022). The adsorption in this type occurs due to interactions between the adsorbate-adsorbent and the adsorbate molecules in the condensed phase. Condensation is the phenomenon of a gas being condensed into a liquid-like phase in the pores (Thahir *et al.,* 2019). Mesoporous silica derived from sugarcane bagasse precursor showed Type H1, showing a narrow pore size distribution (Pingarrón *et al.,* 2020). Type H1 is commonly found in mesoporous silicas with uniform pores, such as MCM-41, MCM-48, and SBA-15 (Pingarrón *et al.,* 2020). In this type, the pore network has minimal influence, resulting in steep, narrow curves, and loops, showing delayed condensation (Kingchok and Pornsuwan, 2020). This showed that mesoporous silica derived from sugarcane bagasse precursor contained interconnected pores forming a network with narrowed pore sizes, resembling an ink bottle shape.

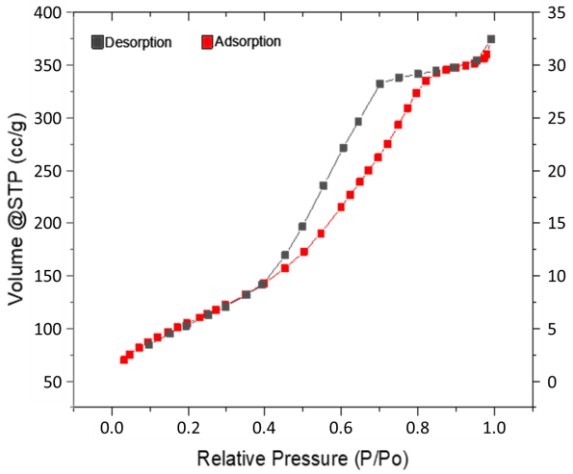

Figure 4 Nitrogen adsorption-desorption isotherm curve for SCBA mesoporous

3.4. Surface Area and Pore Characteristics

BET analysis was conducted on mesoporous silica to determine the surface area and pore characteristics of the tested sample. The results showed that the tested mesoporous

silica had a surface area of 323.297 m^2/g, a pore radius of 24.37 Å, and a pore volume of 0.523 cc/g, as presented in Table 1. The surface area, pore radius, and pore volume characterized using BET were influenced by the mass content of the template used, namely P123 and CTAB (Dhaneswara *et al.,* 2023; Pal, Lee, and Cho, 2020). A previous study showed the significant effect of using CTAB surfactant in decreasing the pore radius. This occurred because CTA+ ion in CTAB-Pluronic system affected hydrophilicity of Pluronic by incorporating the alkyl tail of the cationic surfactant, CTAB, into the polypropylene oxide (PPO) core (Tseng *et al.,* 2017). This leads to a more hydrophilic PPO-PEO interface due to the reduction in PPO volume (Tseng *et al.,* 2017). The presence of H1-type hysteresis loop showed a narrow pore size distribution and uniform particle sizes, observed in the distribution curve presented in Figure 5 (a). This narrow pore size distribution originated from the capillary condensation stage during silica condensation, a process that enhanced the regularity of mesoporous structure and improved its textural properties, such as the pore volume shown in Figure 5 (b) (Thahir *et al.,* 2019).

Table 1 Physical properties of SCBA mesoporous sample obtained from N_2 adsorption measurements

Physical Properties	Value
Surface Area (m^2/g)	323.297 m^2/g
Pore Radius (Å)	24.37 Å
Pore Volume (cc/g)	0.523 cc/g

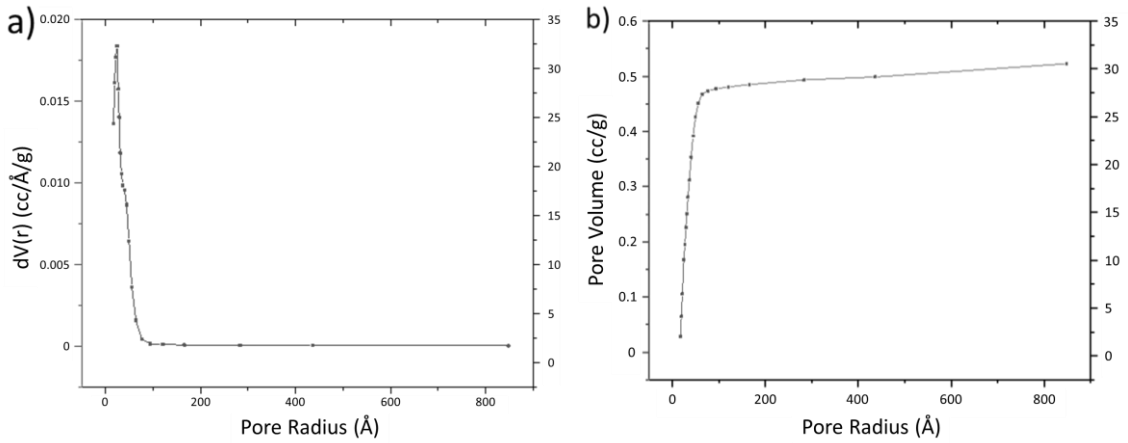

Figure 5 Pore size determination of SCBA mesoporous sample: (a) BJH desorption particle size distribution; (b) the relation between pore size and pore volume

3.5. Identification of Functional Groups

FTIR analysis results showed that peak wavelengths reflected the types of bonds formed in mesoporous silica structure, including O-H, H-O-H, and Si-O-Si groups, as shown in Figure 6. The transmission at peak wavelengths shows the amount of groups formed in mesoporous silica. Moreover, lower transmission at peak wavelengths suggests a higher content of formed groups in mesoporous silica at specific wavenumbers. Table 2 shows the types of bonds formed in mesoporous silica along with the respective transmissions. At a wavenumber of 3401 cm^{-1}, a gradual curve shows the presence of O-H stretching bonds in mesoporous silica (Baumgartner *et al.,* 2019). O-H bonds identified originate from remnants of the precursors that are still present in the pore walls and have not fully decomposed. Another identified group is H-OH functional group at a wavelength of 1633 cm^{-1} related to the water structure, showing the presence of absorbed H-O-H vibration bonds (Baumgartner *et al.,* 2019). H-OH groups originate from water molecules or by-

products of reactions trapped in the Si-O-Si groups (Rashid *et al.,* 2019). Furthermore, the presence of hydroxyl groups, including O-H and H-OH, can enhance the hydrophilic properties and modify the reactivity of the pore channels (Rashid *et al.,* 2019). In mesoporous silica synthesized through the sol-gel process, Si-O-Si groups are divided into three types, namely asymmetric Si-O-Si at a wavenumber of 1072 cm^{-1}, symmetric Si-O-Si at 789 cm^{-1}, and Si-O-Si torque at a 443 cm^{-1}. The formation of Si-O-Si groups, which are the most abundant, shows the success of the sol-gel process in producing mesoporous silica (Purwaningsih *et al.* 2018).

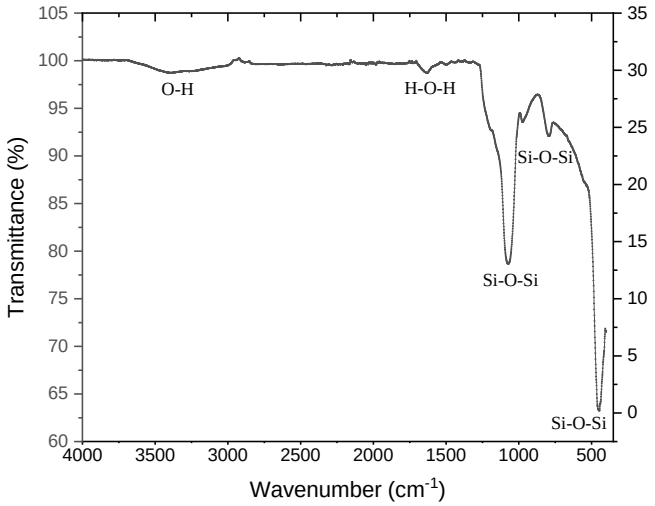

Figure 6 FTIR spectra for SCBA Mesoporous

Table 2 The types of bonds in SCBA Mesoporous

Bonds		SCBA Mesoporous
O-H	Wavenumber (cm^{-1})	3401
	Transmittance (%)	98.7
H-OH	Wavenumber (cm^{-1})	1633
	Transmittance (%)	98.72
Si-O-Si (Asymmetry)	Wavenumber (cm^{-1})	1072
	Transmittance (%)	78.7
Si-O-Si (Symmetry)	Wavenumber (cm^{-1})	789
	Transmittance (%)	92
Si-O-Si (Torque)	Wavenumber (cm^{-1})	443
	Transmittance (%)	63.4

3.6. Adsorption of Methyl Blue

The absorption testing of mesoporous silica for methyl blue solution was conducted for 4 hours with an initial concentration of 10 ppm. Samples of the absorbed mesoporous silica that were synthesized from sugarcane bagasse precursor were taken every hour and compared with the blanco solution. The results of UV-Vis testing for the blanco solution of methyl blue, along with the variation in absorption over time, are presented in Figure 7 (a). In the Blanco solution, the peak with the highest absorbance at a wavenumber of 664 nm and an absorbance intensity of 1.49 nm showed red visible light (Dhaneswara *et al.,* 2020). This red spectrum would reflect the blue color in the increasingly concentrated methyl blue solution (Pratiwi and Nandiyanto, 2022). Furthermore, it was observed that the methyl blue solution absorbed by mesoporous silica has a lower absorbance intensity compared to the blanco solution. The decrease in absorbance intensity at the maximum wavenumber reduces as the absorption time with mesoporous silica adsorbent increases. Based on the results, the sample absorbed for 4 hours has the lowest intensity, reaching 0.0409 AU. The

calculated uptake capacity and %Removal results are presented in Table 3. From the data, synthesized mesoporous silica showed potential as an adsorbent for methyl blue solution. This was evidenced by a %removal exceeding 90% over 4 hours. The adsorption mechanism of methyl blue included the migration of the dye solution to the surface of mesoporous silica due to interactions between adsorbate and adsorbent. Methyl blue, being a cationic dye, would interact electrostatically with the negatively charged silica at normal pH (pH = 7). As presented in Figure 7 (b), the absorption of methylene blue by mesoporous silica for 4 hours resulted in a nearly colorless solution.

Table 3 The result of adsorption uptake capacity and %removal calculation of SCBA mesoporous

Dyes		1 Hour	2 Hours	3 Hours	4 Hours
Methylene Blue	q_t (mg/g)	9	9.4	9.32	9.73
	%Removal	90%	94%	93.20%	97.30%

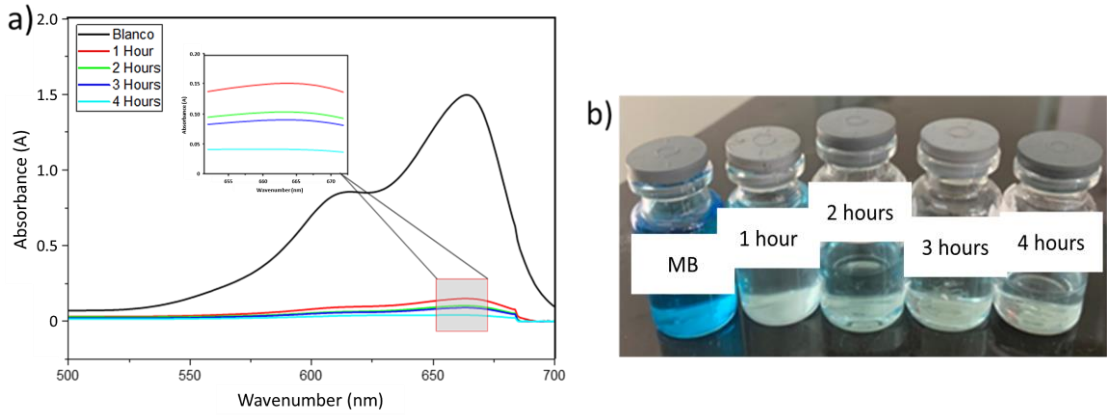

Figure 7 (a) Adsorption Spectra of aqueous methyl blue dye solution in the presence of adsorbent; (b) visual image of aqueous methyl blue dye solution in the presence of adsorbent

4. Conclusions

In conclusion, this study successfully synthesized mesoporous silica material using a precursor derived from sugarcane bagasse, with cationic (CTAB) and non-ionic (P123) surfactant template masses. This process resulted in a two-dimensional body-centered cubic (BCC) crystal structure with Im3m symmetry. The surface morphology of SCBA mesoporous material consisted mostly of spherical particles and some coarse aggregates influenced by the surfactants used. The synthesized material showed a surface area of 323.297 m^2/g, a pore radius of 24.37 Å, and a pore volume of 0.523 cc/g. H1-type isotherm curve suggested a narrow and uniform pore size distribution, contributing to an increased pore volume. FTIR analysis results showed spectra indicating the presence of O-H, H-O-H, and Si-O-Si groups. The presence of three Si-O-Si groups in synthesized mesoporous silica showed the successful sol-gel process. After a 4-hour contact time, SCBA mesoporous material showed the capability to adsorb methyl blue dye with a removal efficiency of 97.3% and an uptake capacity of 9.73 mg/g.

Acknowledgments

This study was supported by a research grant from the Indonesian Ministry of Education, Culture, Research, and Technology No.NKB-1143/UN2.RST/HKP.05.00/2023.

The authors are grateful to the Advanced Materials Laboratory DTMM-FT, Universitas Indonesia.

References

Abboud, M., Sahlabji, T., Haija, M.A., El-Zahhar, A.A., Bondock, S., Ismail, I., Keshk, S.M., 2020. Synthesis and Characterization of Lignosulfonate/Amino-Functionalized SBA-15 Nanocomposites for the Adsorption of Methylene Blue from Wastewater. *New Journal of Chemistry*, Volume 44(6), pp. 2291–2302

Baumgartner, B., Hayden, J., Loizillon, J., Steinbacher, S., Grosso, D., Lendl, B., 2019. Pore Size-Dependent Structure of Confined Water in Mesoporous Silica Films from Water Adsorption/Desorption Using Atr–Ftir Spectroscopy. *ACS Publications,* Volume 35(37), pp. 11986–11994

Bulgariu, L., Bulgariu, D., 2018. Functionalized Soy Waste Biomass - A Novel Environmental-Friendly Biosorbent for the Removal of Heavy Metals from Aqueous Solution. *Journal of Cleaner Production,* Volume 197, pp. 875–885

Dhaneswara, D., Fatriansyah, J.F., Situmorang, F.W., Haqoh, A.N., 2020. Synthesis of Amorphous Silica from Rice Husk Ash: Comparing Hcl and CH3COOH Acidification Methods and Various Alkaline Concentrations. *International Journal of Technology*, Volume 11(1), pp. 200–208

Dhaneswara, D., Marito, H.S., Fatriansyah, J.F., Sofyan, N., Adhika, D.R., Suhariadi, I., 2022. Spherical SBA-16 Particles Synthesized from Rice Husk Ash and Corn Cob Ash for Efficient Organic Dye Adsorbent. *Journal of Cleaner Production*, Volume 357, p. 131974

Dhaneswara, D., Zulfikar, N., Fatriansyah, J.F., Mastuli, M.S., Suhariadi, I., 2023. Adsorption Capacity of Mesoporous SBA-15 Particles Synthesized from Corncobs and Rice Husk at Different CTAB/P123 Ratios and Their Application for Dyes Adsorbent. *Evergreen,* Volume 10(2), pp. 924–930

Fatriansyah, J.F., Situmorang, F.W., Dhaneswara, D., 2018. Ekstraksi silika dari sekam padi: metode refluks dengan NaOH dan pengendapan menggunakan asam kuat (HCl) dan asam lemah (CH3COOH) [Extraction of silica from rice husk: reflux method with NaOH and precipitation using strong acid (HCl) and weak acid (CH3COOH)]. *In*: Prosiding Seminar Nasional Fisika Universitas Riau, Volume 3, pp.123-127

Jawad, A.H., Hum, N.N.M.F., Farhan, A.M., Mastuli, M.S., 2020. Biosorption of methylene blue dye by rice (Oryza sativa L.) straw: adsorption and mechanism study. *Desalin Water Treat*, Volume 190, pp.322-330

Kingchok, S., Pornsuwan, S., 2020. Comparison of Spherical and Rod-Like Morphologies of SBA-15 For Enzyme Immobilization. *Journal of Porous Materials,* Volume 27(5), pp. 1547–1557

Mota, T.L.R., Gomes, A.L.M., Palhares, H.G., Nunes, E.H.M., Houmard, M., 2019. Influence of the Synthesis Parameters on the Mesoporous Structure and Adsorption Behavior of Silica Xerogels Fabricated by Sol–Gel Technique. *Journal of Sol-Gel Science and Technology,* Volume 92(3), pp. 681–694

Nassar, M.Y., Ahmed, I.S., Raya, M.A., 2019. A Facile and Tunable Approach for Synthesis of Pure Silica Nanostructures from Rice Husk for the Removal of Ciprofloxacin Drug from Polluted Aqueous Solutions. *Journal of Molecular Liquids,* Volume 282, pp. 251–263

Pal, N., Lee, J.H., Cho, E.B., 2020. Recent Trends in Morphology-Controlled Synthesis and Application of Mesoporous Silica Nanoparticles. *Nanomaterials,* Volume 10(11), pp. 2122

Pingarrón, J.M., Labuda, J., Barek, J., Brett, C.M.A., Camões, M.F., Fojta, M., Hibbert, D.B., 2020. Terminology of Electrochemical Methods of Analysis (IUPAC Recommendations 2019). *Pure and Applied Chemistry,* Volume 92(4), pp. 641–694

Pratiwi, R.A., Nandiyanto, A.B.D., 2022. How to Read and Interpret UV-VIS Spectrophotometric Results in Determining the Structure of Chemical Compounds. *Indonesian Journal of Educational Research and Technology*, Volume 2(1), pp. 1–20

Purwaningsih, H., Pratiwi, V.M., Purwana, S.A.B., Nurdiansyah, H., Rahmawati, Y., Susanti, D., 2018. Fabrication of Mesoporous Silica Nanoparticles by Sol Gel Method Followed Various Hydrothermal Temperature. *AIP Conference Proceedings,* Volume 1945(1), pp. 1–8

Rashid, R., Afroze, F., Ahmed, S., Miran, M.S., Bin, A., Susan, H., 2019. Control of the Porosity and Morphology of Ordered Mesoporous Silica by Varying Calcination Conditions. *Materials Today: Proceedings,* Volume 15, pp. 546–554

Raya, I., La Nafie, N., Thahir, R., Yasser, M., Ismail, S., 2021. Prepare and utilize mesoporous silica SBA-15 for efficient photocatalytic adsorption of methylene blue and copper (II). *Journal of Physics: Conference Series*, Volume 2049(1), pp. 012083

Shah, B.A., Patel, A. V, Bagia, M.I., Shah, A. V, 2017. Green Approach towards the Synthesis of MCM-41 from Siliceous Sugar Industry Waste. *International Journal of Applied Chemistry,* Volume 13(3), pp. 497–514

Sohrabnezhad, S., Jafarzadeh, A., Pourahmad, A., 2018. Synthesis and Characterization of MCM-41 Ropes. *Materials Letters,* Volume 212, pp. 16–19

Sudibandriyo, M., Putri, F.A., 2020. The Effect of Various Zeolites as an Adsorbent for Bioethanol Purification Using a Fixed Bed Adsorption Column. *International Journal of Technology,* Volume 11(7), pp. 1300–1308

Szewczyk, A., Prokopowicz, M., 2020. Mesoporous Silica Pellets–A Promising Oral Drug Delivery System? *Journal of Drug Delivery Science and Technology*, Volume 56, pp. 101491

Thahir, R., Wahab, A.W., Nafie, N. La, Raya, I., 2019. Synthesis of High Surface Area Mesoporous Silica SBA-15 By Adjusting Hydrothermal Treatment Time and the Amount of Polyvinyl Alcohol. *Open Chemistry,* Volume 17(1), pp. 963–971

Thu, H.T., Dat, L.T., Tuan, V.A., 2019. Synthesis of mesoporous SiO2 from rice husk for removal of organic dyes in aqueous solution. *Vietnam Journal of Chemistry*, Volume 57(2), pp.175-181

Tseng, H.H., Chuang, H.W., Zhuang, G.L., Lai, W.H., Wey, M.Y., 2017. Structure-controlled Mesoporous SBA-15-Derived Mixed Matrix Membranes for H2 Purification and CO2 Capture. *International Journal of Hydrogen Energy*, Volume 42(16), pp. 11379–11391

Wang, Y., Zhuang, Y., Wang, S., Liu, Y., Kong, L., Li, J., Chen, H., 2022. Preparation and Characterization of Porous Palygorskite/Carbon Composites through Zinc Chloride Activation for Wastewater Treatment. *Clays and Clay Minerals,* Volume 70(3), pp. 450–459

Wilson, L.D., Mahmud, S.T., 2015. The Adsorption Properties of Surface-Modified Mesoporous Silica Materials with ß-cylodextrin. *International Journal of Technology,* Volume 6(4), pp. 533–545